Int J Adv Manuf Technol (2015) 78:927–937
DOI 10.1007/s00170-014-6691-9

ORIGINAL ARTICLE

Virtual tryout and optimization of the extrusion die for an aluminum profile with complex cross-sections

Cunsheng Zhang · Guoqun Zhao · Yanjin Guan · Anjiang Gao · Lanjun Wang · Peng Li

Received: 18 September 2014 / Accepted: 1 December 2014 / Published online: 23 December 2014

Abstract In this paper, the "trial-and-repair" process of the extrusion die is transferred from the workshop to the computer for a complex hollow aluminum profile used in high-speed trains. Firstly, a finite element (FE) model of the extrusion process is established with the arbitrary Lagrangian–Eulerian code HyperXtrude. To balance the material flow velocity in the die cavity, more than ten baffle plates are used and distributed in the welding chamber. Then, taking the exit velocity uniformity as the evaluating criterion, the initial extrusion die is modified by adjusting the shapes, the layout, and the heights of the baffle plates. Through a series of modifications, the velocity difference in the cross-section of the extrudate decreases significantly from 102.3 mm/s with the initial die to 26.6 mm/s with the final one. The local twisted or bent deformation of the extrudate is well controlled with the optimal die. Finally, a real extrusion die is manufactured and a practical profile is extruded. The difference in the rib thickness of the profile between the experimental measurements and desired dimensions is 0.12 mm, which satisfies the practical requirements. Moreover, the microstructures in the profile and its ribs are examined, and no heat defects are observed in the profile. Therefore, the virtual tryout of the extrusion die in this work are well verified, and the design rules of extrusion dies could provide theoretical guidance for practical repairs of complex extrusion dies in workshop.

Keywords Virtual tryout · Porthole die · Die modification · Aluminum profile extrusion

C. Zhang · G. Zhao (✉) · Y. Guan
Key Laboratory for Liquid–Solid Structural Evolution & Processing of Materials (Ministry of Education), Shandong University, Jinan, Shandong 250061, People's Republic of China
e-mail: zhaogq@sdu.edu.cn

C. Zhang
e-mail: zhangcs@sdu.edu.cn

C. Zhang · A. Gao · L. Wang
Conglin Aluminum Co., Ltd., Yantai, Shandong 265705, People's Republic of China

P. Li
CSR Qingdao Sifang Co., Ltd, Qingdao, Shandong 266111, People's Republic of China

1 Introduction

Currently, aluminum alloy profiles have been widely applied in many fields such as rail transportation, aerospace, marine, construction, infrastructure, and other sectors due to their attractive combination of good mechanical properties, high corrosion resistance, high extrudability and formability, good surface appearance, etc. [1].

During the production of aluminum alloy profiles, proper die design is an important factor to produce high-quality products with good mechanical properties and microstructures, especially for large complex aluminum profiles used in high-speed trains. However, until now, designing a die has been mainly based on empirical knowledge and the experience of the die designer, and many times of "trial-and-repair" process are usually carried out before a good product is produced. To reduce the wasted scrap and time in these trial-and-error iterations, much attention has been recently drawn on the application of numerical analysis to gain more insight in the extrusion process [2–16].

Lee et al. [3] have simulated the porthole die extrusion process for producing condenser tubes used for cooling systems of automobiles. The effects of chamber shape on the material flow, welding pressure, extrusion load, and the tendency of mandrel deflection have been evaluated. Research regarding the effect of pocket dies on multi-hole die extrusion was performed by Peng and Shepard [4]. Based on three-dimensional FE calculations, they concluded that balanced

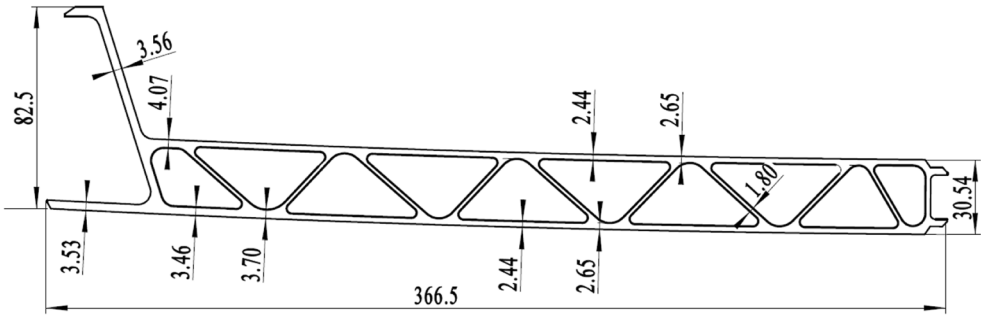

Fig. 1 Cross-section shape and main dimensions of the profile (mm)

material flow and temperature distribution as well as structural homogeneity of the extrudates can be achieved by a suitable location of the pockets. Even a small offset of a pocket can cause a significant change in the metal flow during the extrusion process and reduce the quality of the extrudates. Kloppenborg et al. [5] developed a modular die concept to analyze the viscoplastic material flow distribution inside a porthole die extrusion process. It was found that material inside the feeder geometry sheared in a layer area near the die wall, while outside this area the material flowed at constant velocity. In addition, the experimental data was also used to verify the numerical analysis with HyperXtrude and Deform3D. Carmai et al. [6] have investigated the influence of offset pocket design on metal flow behavior in hot aluminum extrusion by keeping a single bearing length. It was found that small distance between the edge of the pocket and the edge of the die leads to low flow velocity. If the distance is large, however, the metal can flow through more easily, and the velocity is higher. Finally, a new optimum pocket was proposed. Donati et al. [7] investigated metal flow in a multi-hole die with four L-shaped openings, four different pocket shapes, and two different profile thicknesses (2 and 3 mm, respectively). Experimentally, it was found that at low production rates, a conical pocket resulted in a lower exit speed than a stepped one, while the classical centered pocket gave much faster flow than the non-centered one. By use of DEFORM-3D, He et al. [8] have investigated the effects of pockets in a two-hole extrusion die on the metal flow, the temperature, and the extrusion load. The simulation results showed that the pocket could be used to effectively adjust the metal flow, especially to benefit the metal flow under the legs. Fang et al. [9] investigated the effect of pocket shape on metal flow by extrusion of U-shaped profiles with different wall thicknesses through a multi-hole pocket. Chen et al. [10] investigated the effects of the step of the welding chamber on the metal flow and the die strength for a hollow profile. They found that with an increased step of the welding chamber, more uniform velocity and temperature distributions were obtained. In addition, the weld quality was improved due to increased welding pressure when using the multi-step welding chamber. Moreover, with an increased step of welding chamber, the maximum stress and the deflection of the lower die decreased, while the deflection of the mandrel was almost unchanged and the maximum stress of upper die increased [11]. Zhang et al. [12] have obtained an optimal die structure for a three-cavity profile by adjusting the layouts, shapes, and heights of the baffle plates in the welding chamber. Finally, a sound profile was produced. Li et al. [13] studied the metal flow behavior in the extrusion process with inner cone punch by numerical simulation and experiment, and concluded that inner cone punch was beneficial to the extrusion process and the promotion of product quality. Rout and Maity [14] obtained the optimum die length for extrusion of square sections from a square billet by using three-dimensional upper bound method, and the proposed die shape profile was found to be superior to many other profiles by experiments. Hwang and Chen [15] investigated the effect of the die inclination angle on surface permeation during a rod extrusion, and determined the optimal inclination angle to minimize surface permeation and achieve optimal product ratios. By resizing portholes, adding bosses, chamfering mandrels, and adjusting the length of the bearings, Liu et al. [16] balanced the local metal flow velocity effectively during the extrusion of a multi-cavity aluminum profile and achieved high-quality products.

From state-of-the-art analysis, many scholars have carried out investigations on extrusion processes for aluminum profiles and obtained optimum extrusion dies; however, most research has been focused on the profiles with simple cross-sections or thick wall profiles. During the production of complex and multi-cavity aluminum profiles used in high-speed

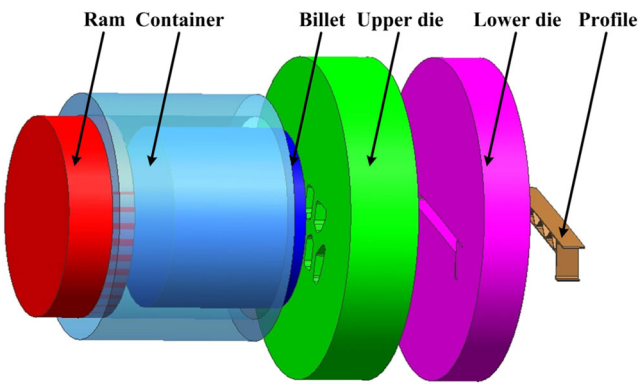

Fig. 2 Assembly drawing of general extrusion tool components

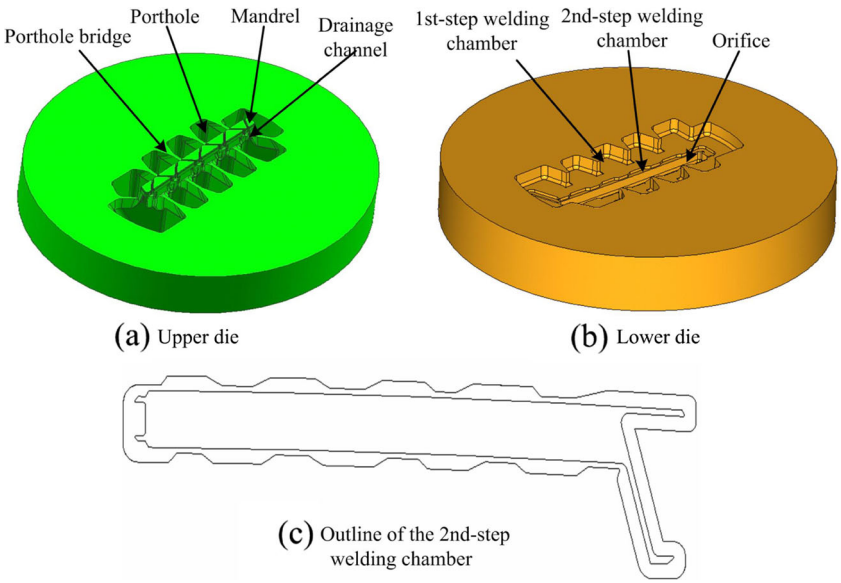

Fig. 3 Extrusion die initially designed for producing the profile

trains, the material flow in die cavity is very complicated and practical "trial-and-repair" process of the extrusion dies is greatly time-consuming in the workshop. Therefore, to reduce the trial-and-error iterations and improve the product quality, in this work, the trial-and-error process of the extrusion die will be transferred from the workshop to the computer. By distributing and adjusting the layout, shapes, and heights of baffle plates in the welding chamber, material flow will be analyzed and an optimal extrusion die will be obtained. Then, a real die will be manufactured and a practical profile extrusion will be extruded on an 80 MN extrusion machine. Finally, the geometry size and microstructure of the produced profiles will be examined.

2 Numerical modeling of extrusion process

2.1 Construction of geometry models

The cross-section shape and main dimensions of the hollow profile in this study are shown in Fig. 1. The profile had a maximum length of 366.5 mm and ten cavities, with maximum and minimum wall thickness levels at 4.07 and 1.8 mm, respectively. Due to its complex cross-section shape, large width-to-thickness ratio, and large difference in wall thickness, the material flow during extrusion is extremely complex, which makes it difficult to guarantee that all points in the cross-section of the profile flow out of the die orifice with an identical velocity.

The porthole die assembly is shown in Fig. 2, consisting of a ram, a container, an upper die, and a lower die, which is designed for producing this kind of aluminum profiles. The initial die structure is shown in Fig. 3. Figure 3a is the upper die, with an outer diameter of 700 mm and a height of 203 mm. In order to reasonably control the material distribution and balance the material flow, ten portholes are designed. In addition, drainage channels are adopted between adjacent mandrels to guide material flowing into the ribs, where it is very difficult to form for this complex profile. The lower die with an outer diameter of 700 mm and a height of 115 mm is shown in Fig. 3b. In order to better control the material

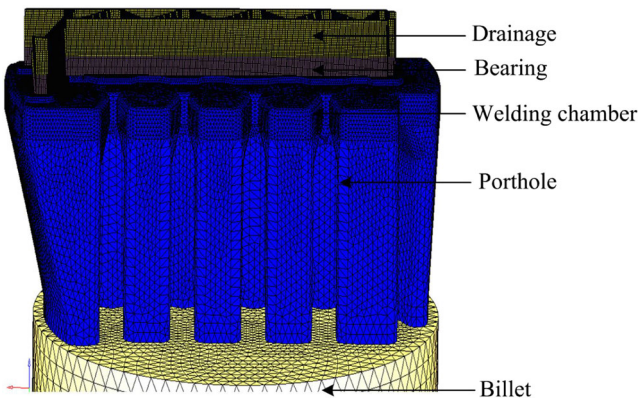

Fig. 4 Numerical model for metal flow analysis

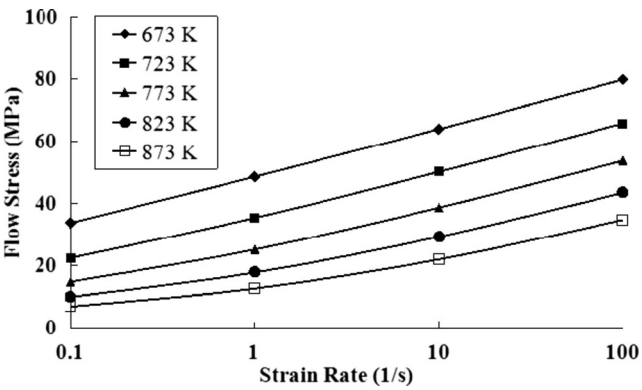

Fig. 5 Flow stress curve of AA6005 at different temperatures and strain rates

Table 1 Mechanical properties of AA6005 and H13

Material	Young's modulus (Pa)	Poisson's ratio	Density (kg/m^3)	Thermal conductivity (N/(s K))	Specific heat (N/(mm^2 K))
AA6005	4.0E+10	0.35	2700	180	896
H13	2.1E+11	0.35	7870	24.3	460

distribution, a two-step welding chamber is initially used in the lower die. The heights of the first-step and second-step welding chambers are 25 and 5 mm, respectively, where the latter is more similar to the cross-section of the profile, as shown in Fig. 3c.

2.2 Mesh model

To simulate the extrusion process with HyperXtrude, all the regions that material flows through should be extracted and then meshed. The numerical model for flow analysis is shown in Fig. 4, of which the mesh number is about 1,900,000 with finer triangular prism elements that are assigned in the regions of bearing and profile and relatively coarse tetrahedral elements in other regions.

2.3 Material parameters

The billet consisted of AA6005 aluminum alloy with medium strength, heat treatability, and excellent corrosion resistance. Here, the Sellars–Tegart equation is used to describe the high-temperature behavior of AA6005 [17] and given by:

$$\sigma = \frac{1}{\beta}\sinh^{-1}\left(\frac{Z}{A}\right)^{1/n} \tag{1}$$

Here σ is the flow stress; β, n, and A are the temperature-independent material parameters; and Z is the Zener–Hollomon parameter, defined by

$$Z = \dot{\bar{\varepsilon}} e^{Q/RT}, \tag{2}$$

where $\dot{\bar{\varepsilon}}$ is the effective strain rate, Q is the activation energy, R is the universal gas constant, and T is the absolute temperature. Parameters values used for AA6005 in this work are [18] $Q=1.648\times10^5$J/mol, $R=8.314$ J/(mol·k), $A=7.55\times10^{10}$s^{-1}, $n=3.649$, and $\beta=3.96\times10^{-8}$m^2/N.

The flow stress curve of AA6005 at varying temperatures (approximately 673–873 K) and varying strain rates (approximately 0.1–100 s^{-1}) is shown in Fig. 5.

H13 steel is widely used as die material due to its high abrasion resistance, high hardness, and low sensitivity to heat checking. The mechanical properties of AA6005 and H13 are given in Table 1.

2.4 Process parameters

In the numerical simulation, a cylinder billet with a diameter of 400 mm and a height of 800 mm is used. The extrusion ratio (defined as the cross-section area of the billet divided by the cross-section area of the final profile) is found to be 42.6, indicating that this profile is a hard-to-form one. According to the material characteristic of AA6005, the billet temperature and tooling temperature are chosen as 773 and 753 K, respectively. The heat convection coefficient between the die and the billet material is 3000 W/m^2·K. The ram speed is 1.0 mm/s. The process parameters used in simulation are given in Table 2.

During the extrusion process, the aluminum billet is in direct contact with the container and die manufactured in hot-working steel H13. At elevated temperature, there is significant adhesion between billet and extrusion die. To describe the friction behavior, the sticking condition is used for all interfaces between the billet and the tooling (container and die) except at the die bearing land. At the die bearing land, a Coulomb friction factor of 0.3 is prescribed, so as to simplify the complex interfacial conditions ranging from full sticking at the die entrance to slipping at the end of the bearing. The numerical simulation of the aluminum profile extrusion takes almost 20 h on a Linux workstation for the model described above.

Table 2 Definition of process parameters in the simulation

Billet diameter (mm)	Billet length (mm)	Extrusion ratio	Initial temperature of billet (K)	Initial temperature of tool (K)	Heat convection coefficient (W/m K)	Ram speed (mm/s)
400	800	42.6	773	753	3000	1.0

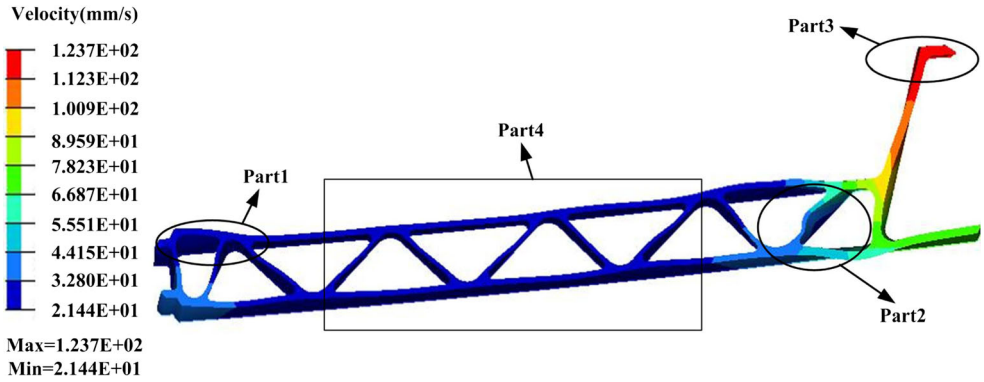

Fig. 6 Velocity distribution in the cross-section with the initial extrusion die

3 Numerical simulation and result analysis

A large variety of information can be obtained from the numerical simulation, such as velocities, strains, stresses, temperatures, and extrusion forces. The velocity distribution in the cross-section of the profile is shown in Fig. 6. It is seen that severe twist deformation occurs due to the non-uniform metal flow. The maximum velocity is up to 123.7 mm/s (Part 3), while the minimum one is only 21.4 mm/s (Part 4). During the extrusion process, the regions with high flow velocity continuously squeezes those with low velocity, which makes the extrudate bent and twisted, especially in Parts 1 and 2. Therefore, some adjustments should be taken to optimize the initial die design and balance the material flow in the extrusion process.

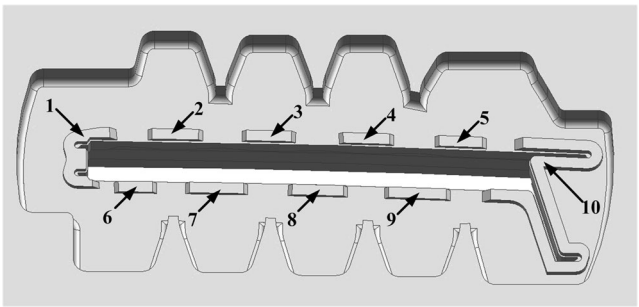

Fig. 7 Layout and shapes of baffle plates in the first modification scheme

The large velocity difference in the cross-section of the profile could be explained as follows: (1) Part 3 is entirely under the die portholes, which is similar to the flat die extrusion. Consequently, material flows out of the portholes directly to form this part subjected to less resistance, so material flows faster in the part than other parts. (2) In order to gain the final shape of the sections under the port bridge, the material has to overcome the additional friction resistance between the material and the port bridges. In addition, the metal streaming from the neighboring portholes will be rewelded under the port bridge. As a result of severe collision of two metal streams, the flow velocity will be partially counteracted. (3) To form the ribs of the profile, the material should change its flow direction into the drainages and finally be forced to flow out of the die orifice. In the whole forming process, the material flow is very complex, especially in the drainage channels, where material flow resistance is great. It is because of a lack of material supply the ribs were usually relatively low velocity and consequently the dimension of ribs is obviously less than standard size.

In a real extrusion process, the uniformity of the flow velocity distribution at the die exit greatly influences the quality of the extrudate. To describe the degree of the velocity uniformity in the cross-section of the extrudate, the function–

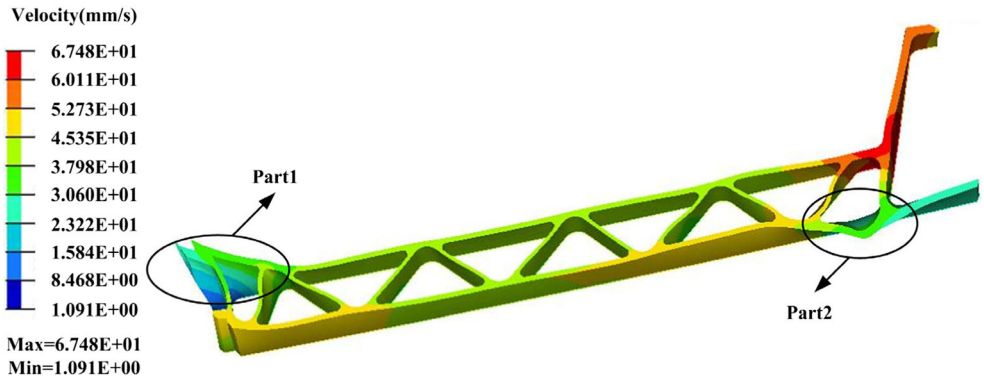

Fig. 8 Velocity distribution in the cross-section with the first optimum extrusion die

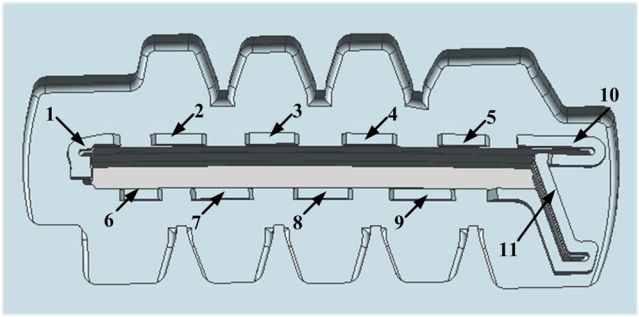

Fig. 9 Layout and shapes of baffle plates in the second modification scheme

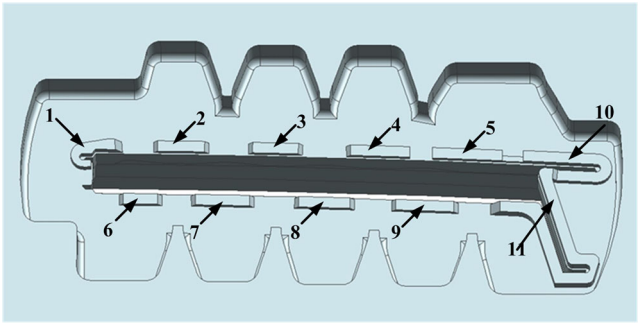

Fig. 11 Layout and shapes of baffle plates in the third modification scheme

VRD (Velocity Relative Difference) is introduced and given by:

$$\mathrm{VRD} = \frac{\sum_{i=1}^{n} \frac{|v_i - v_a|}{v_a}}{n} \times 100\% \quad (3)$$

where v_i is the velocity at node i in the cross-section, v_a is the average velocity of all nodes considered, and n is the number of nodes considered. The smaller the VRD value, the better the quality of extruded profile. To get a more practical velocity distribution, all nodes in the cross-section of the profile in Fig. 6 are considered and their velocities are recorded. After calculation, the VRD in the cross-section of the extrudate for the initial die design is found to be 40.7 %.

According to the above analysis and the problems of the initial die design, even though the two steps of welding chamber are designed to balance the material supply, severely non-uniform material flow still occur in the cross-section of the extrudate. In the following, the baffle plates are set to replace the second-step welding chamber and to force the material into the hard-to-deform parts.

4 Modification of the extrusion die

4.1 First modification scheme

In order to balance the metal flow, the second-step welding chamber is removed and the baffle plates are added in the welding chamber. A higher or wider baffle plate is designed in the welding chamber where the metal flow velocity is greater, while no baffle plate or a lower one is used in the welding chamber where the part is particularly difficult to form. Consequently, the material flow resistance could be changed to make the metal flow velocity more uniform in the cross-section of the extrudate. In the first modification scheme, ten baffle plates are used. The layout and the shapes are shown in Fig. 7. The heights of Baffle Plates 1 and 10 are 5 and 6 mm, respectively, while others are 3 mm in height.

The extrusion process is simulated again with the same process parameters as in the initial process. The flow velocity distribution is shown in Fig. 8. The velocity distribution differs largely from the initial one, and the velocity difference in the cross-section of the extrudate is reduced from 102.3 to 66.0 mm/s. Due to much more material supply in the ribs, a significant improvement of the flow velocity could be observed. However, severe deformation still occurs in Parts 1 and 2. The phenomenon is explained as follows: Baffle Plate 1

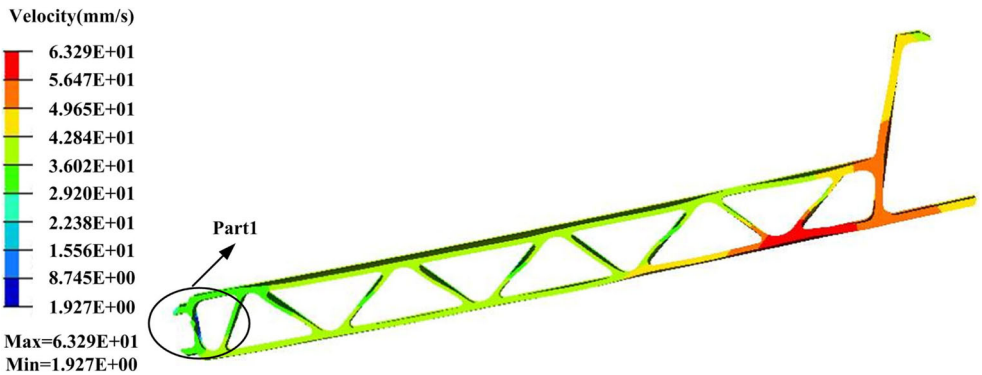

Fig. 10 Velocity distribution in the cross-section with the second optimum extrusion die

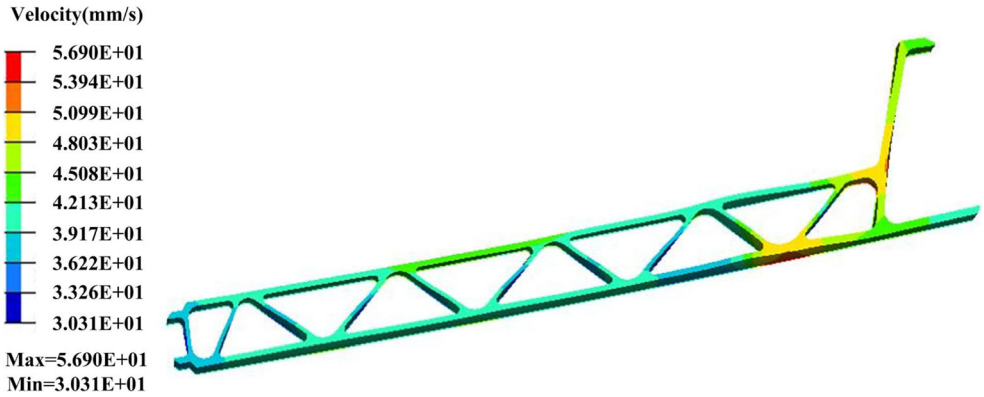

Fig. 12 Velocity distribution in the cross-section with the third optimum extrusion die

and Baffle Plate 10 lead to greater material flow resistance and lower flow velocity. Consequently, Parts 1 and 2 are continuously squeezed by adjacent regions with high flow velocity.

4.2 Second modification scheme

The second modification of the baffle plates mainly focuses on the local deformation in Parts 1 and 2. In this modification scheme, Baffle Plate 10 is divided into two parts; the heights of Baffle Plates 10 and 11 are 4 and 7 mm, respectively. In addition, the shape of Baffle Plate 1 is changed, while the others are kept the same as in the first modification. The layout and the shapes of the baffle plates are shown in Fig. 9. Figure 10 shows the flow velocity distribution in the cross-section after the second modification. It is seen that severe local deformation that occurs in Fig. 8 disappears. However, due to Baffle Plate 1, there is still local distortion around Part 1. In addition, non-uniform thickness is distributed in the cross-section of the profile, especially in the ribs. The VRD is found to be 13.0 % and great velocity difference (61.4 mm/s) still exists.

4.3 Third modification scheme

According to the results of the second modification, the shape of Baffle Plate 1 is changed in this modification scheme, as shown in Fig. 11. Through numerical simulation of the extrusion process, the velocity distribution in the cross-section of the profile is obtained as shown in Fig. 12. It is seen that relatively uniform flow velocity is distributed in the cross-section with a maximum velocity of 56.9 mm/s and a minimum velocity of 30.3 mm/s. The VRD is found to be 6.3 %, and there is 84.5 % decrease in VRD from 40.7 % in the initial simulation. The local deformation is also well controlled, and due to sufficient material supply in the ribs, the shape and size of the profile basically satisfy the practical requirements, as shown in Fig. 12. In the following, the metal flow behavior, the die stress, and the deflection distribution will be investigated on the basis of this optimum die structure.

5 Result analysis for optimum die design and discussion

5.1 Metal flow analysis

Figure 13 shows the velocity distribution of the four sections (or moments) extracted from the inlet of the portholes to the die exit along the extrusion direction, which reflects the status of the metal flow in the whole extrusion process.

Figure 13a shows the velocity distribution on a specified plane at the entrance of the portholes. It is seen that metal flow velocity decreases gradually from the center to its periphery

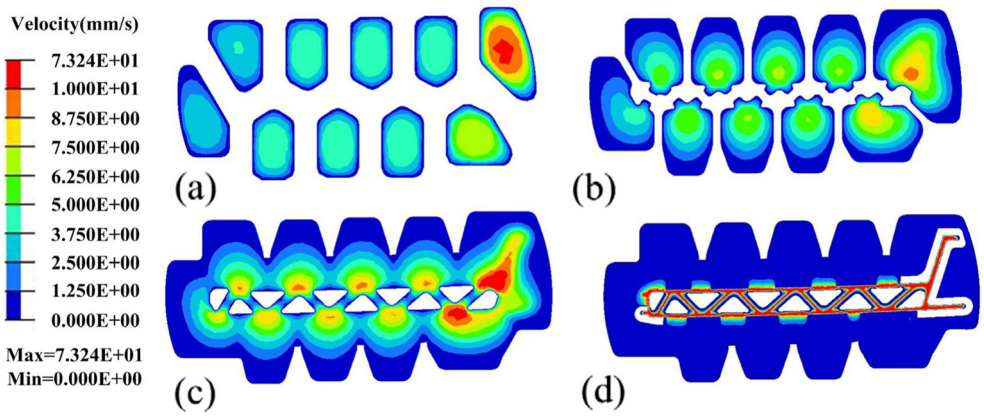

Fig. 13 Metal flow analysis in die cavity during the extrusion process

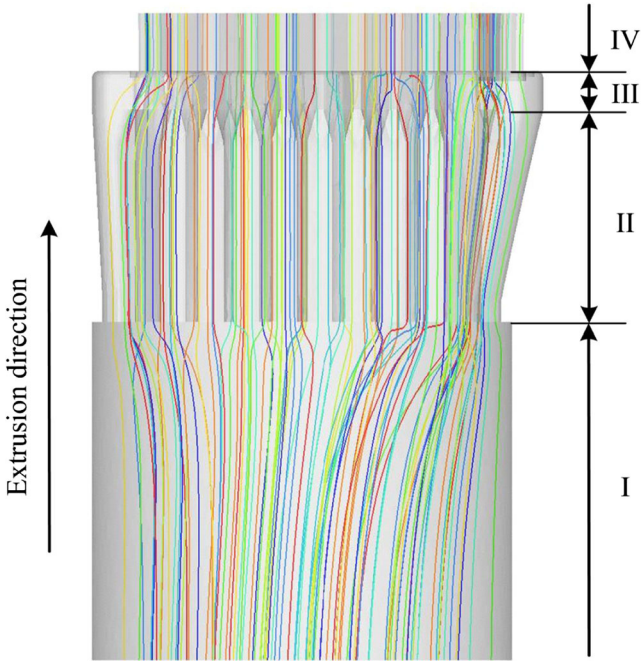

Fig. 14 Plot of metal particles in the whole extrusion process

for every porthole due to the strong friction (sticky condition) on the porthole wall.

Figure 13b shows the velocity distribution at the inlet of the drainage channels. In this stage, one part of the material continues to flow into the die orifice along the extrusion direction, while the other flows into the ribs through the drainage channels. Thus, sufficient material flows into the drainage channels for forming ribs of the profile, which are difficult to form.

Figure 13c shows the status of the metal flow in the welding chamber. It can be seen that metal under the bridges are rewelded further and the metal flow in the welding chamber tends to be more uniform.

Figure 13d shows the velocity distribution at the inlet of the die orifice. At this moment, the flow velocity reaches the peak. The metal flow at the die exit is regulated by the bearing land and the final shape of the extrudate is obtained.

A tracking plot of metal particles for the whole extrusion process is shown in Fig. 14. According to the flow paths of metal particles, the extrusion process can be divided into four stages.

In the first stage, the ram begins to contact the billet and forces it to fill the gap between the billet and the container. The extrusion process is similar to the cylinder upsetting, where metal flows mainly along the radial direction. Due to the slight material deformation in this stage, the metal flow is very regular. At the end of this stage, the material is split into distinct streams. Therefore, the metal begins to flow in disorder.

In the second stage, the metal is forced to fill out the portholes. This forming stage is similar to the direct extrusion process, where metal in the portholes is deformed only by rigid displacement, while shear friction occurs for the metal in contact with the die cavity. Thus, metal flows regularly at this stage.

In the third stage, the metal arrives at the welding chamber and begins to radial upsetting until the metal streams are welded completely under high pressure. Then the metal begins to change the flow direction and to flow into the die orifice. It is seen that some broken lines appear. This is because at this moment, the material encounters the baffle plates in the welding chamber, and it must change its flow direction to bypass the baffle plates. Thus, material is forced to flow into the hard-to-deform parts of the profile. At the same time, due to the baffle plates, new dead zones will occur.

In the fourth stage, the metal begins to flow out through the die bearing. In this stage, severe deformation occurs and the required extrusion load rises rapidly to maximum until the nose end of the profile is extruded out of the die orifice with regular particle lines.

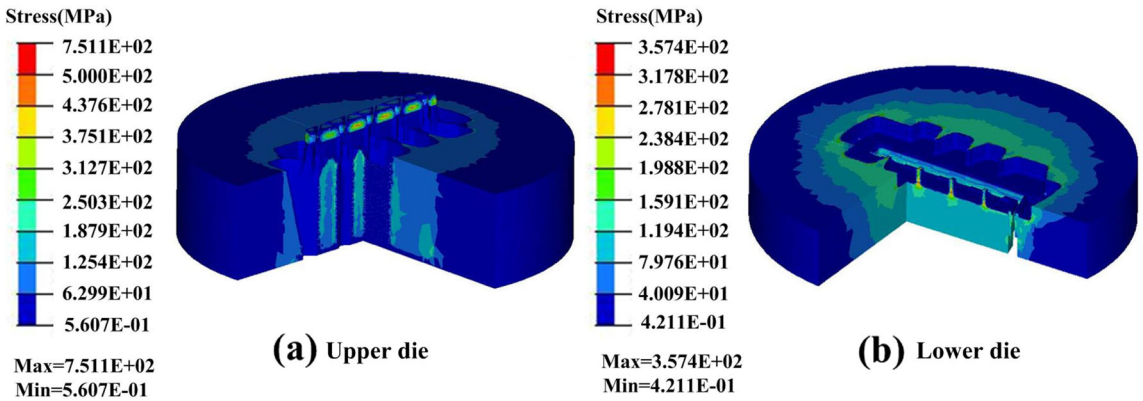

Fig. 15 Stress distribution on the extrusion die

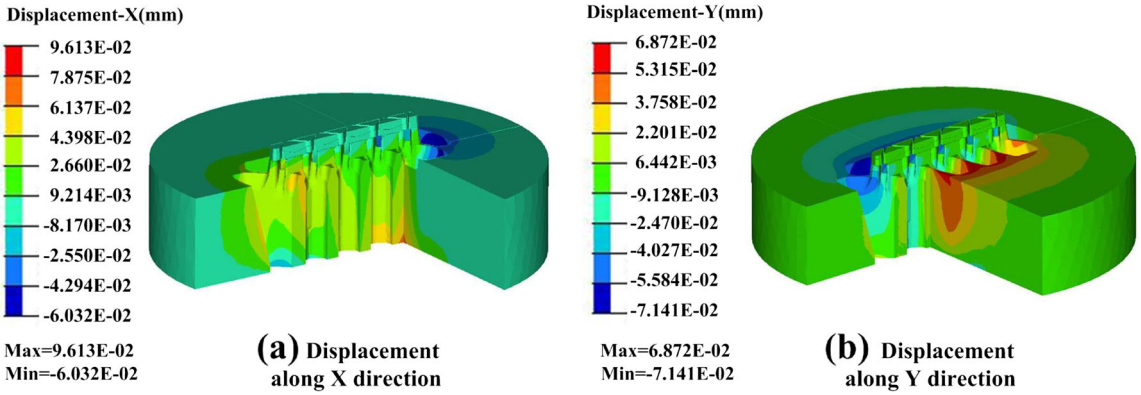

Fig. 16 Displacements along *X* and *Y* direction of the upper die

5.2 Die strength and deflection analysis

In practice, the extrusion die usually works in a severe environment with high temperature, high pressure, and high friction, which easily causes the porthole die to be abandoned owing to plastic deformation and cracking. Therefore, it is necessary to carry out strength checking for extrusion dies.

Figure 15 shows the stress distribution in the extrusion die. Greater stress occurs in the upper die than in the lower die, mainly in the die mandrel. The maximum stress reaches the value of 750 MPa in the mandrel, which is less than the yield strength of H13 (834 MPa at 873 K). Thus, the extrusion die could bear the severe working conditions during the extrusion process and meet the practical production requirements.

In addition, most attention has been paid to the die deflection along the extrusion direction (*Z* direction). However, it is found in practical production that the excessive die deflections in the *X* and *Y* directions easily lead to die failure, which cannot be found by investigating the die deflection along the *Z* direction. In practice, the deflection of the extrusion die along the extrusion direction (*Z*) could be compensated by means of increasing the length of the bearing on the mandrel or the die orifice. Therefore, in this work, only die displacements along the *X* and *Y* directions are investigated to check whether the deflection of the die is acceptable.

Figures 16 and 17 show the deflection distributions along the *X* and *Y* directions in the upper and lower dies. The maximum displacements of the upper die along the *X* and *Y* directions are 0.096 and 0.069 mm in the upper die, respectively, while the corresponding values of the lower die are 0.044 and 0.068 mm, respectively. Therefore, the deflections in the upper and lower dies are slight with an order of magnitude of 10^{-2} mm, which is marginal and almost negligible. As plastic deformation in the extrusion die does not occur, the extrusion die could be put into practical production.

5.3 Discussion

By adjusting the layout, the shape, and the height of the baffle plates, metal flow could be effectively controlled and material supply in ribs could be ensured. Finally, a profile with desired shape and precision size is obtained.

However, there is 5.4 % increase in the required extrusion force of the optimum die (65.25 MN) in comparison with that of the initial one (61.93 MN). This is because of the use of the baffle plates in the optimum die leading to increased material

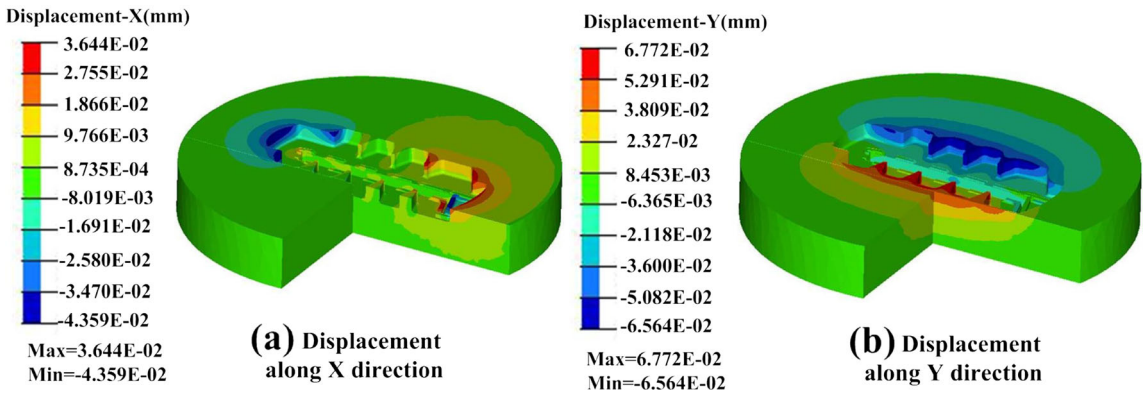

Fig. 17 Displacements along *X* and *Y* direction of the lower die

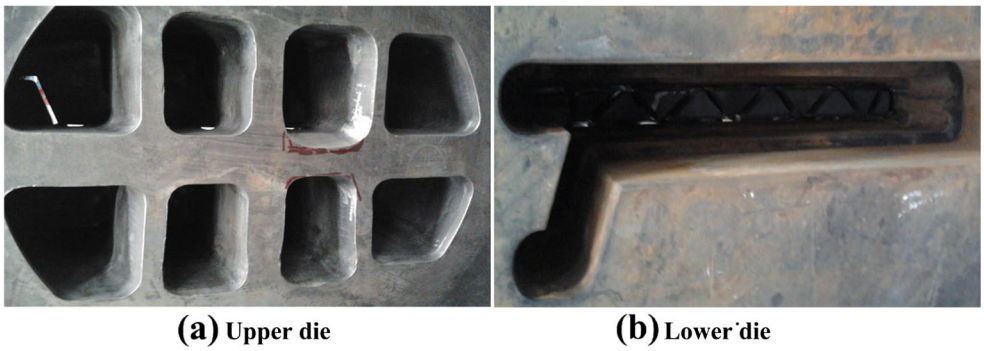

Fig. 18 Extrusion die in the experiment

flow resistance. Considering the safety allowance, this extrusion process could be carried out on an 80 MN extrusion press.

6 Experimental verification and analysis

According to the optimum extrusion die obtained by the above procedure, a real extrusion die is manufactured and a practical profile extrusion is accomplished on an 80 MN extrusion machine. The porthole structure and die orifices are shown in Fig. 18. The temperature of initial billet and die, billet diameter, and ram speed are all under close control in order to duplicate the conditions of the FE simulations. Figure 19 shows the produced profile. No distinct twist or bent deformation in the cross-section was found. Moreover, the rib thicknesses of the profile are also measured, as shown in Fig. 20. The maximum difference between experimental and required thicknesses of the ribs is 0.12 mm, which satisfies the engineering requirements.

For practical application, attention must be taken again to avoid overheating, as this is detrimental to the aluminum profile. Figure 21 shows the grain microstructures on the profile and its ribs. According to the analysis, there do not exist remelting eutectics, local remelting that widens the grain boundaries, and remelting triangles in the intersection of three grains, which are the criteria to judge whether the overheated structure occurs. Therefore, overheat phenomena do not occur in the test samples.

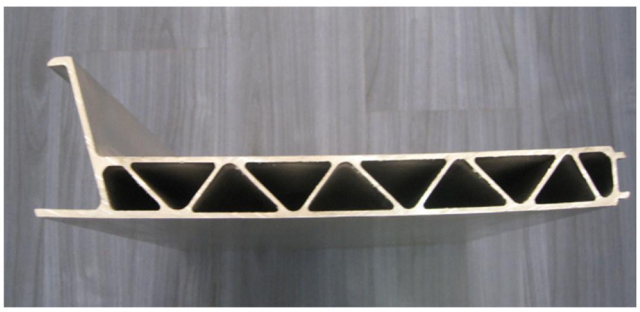

Fig. 19 Profile manufactured in real production

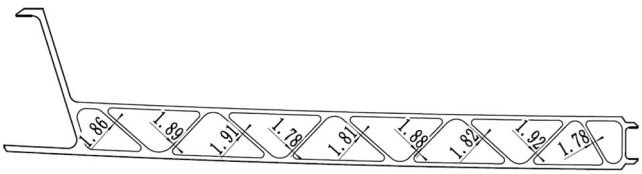

Fig. 20 Rib thicknesses of the profile extruded in the work

7 Conclusions

In this paper, the extrusion process of a complex cross-section and thin-walled aluminum profile used for high-speed trains has been investigated numerically and experimentally. By adjusting the layout, shape, and height of baffle plates, a profile with desired shape and precision size has been obtained. Through a series of numerical simulations and experimental verifications, the following conclusions are drawn.

1. Baffle plates play a more efficient role in balancing metal flow and material distribution than the second-step welding chamber during the extrusion process of large

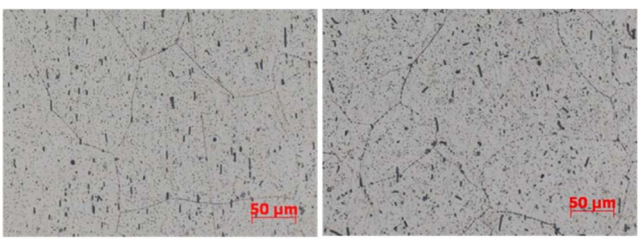

(a) Grain microstructure of profile (b) Grain microstructure in ribs

Fig. 21 Grain microstructure of the profile and in its ribs

and complex profiles. By optimizing the baffle plates in the welding chamber, the metal flow velocity in the cross-section of the profile at the die exit tends to be more uniform. The VRD is found to be 6.3 % with the optimum die scheme, and there is 84.5 % decrease in VRD from 40.7 % by the initial die scheme.

2. On the basis of the optimum extrusion die, metal flow behavior, die stress, and deflection have been investigated numerically. By tracking the plot of metal particles for the whole extrusion process, the extrusion process is clearly divided into four forming stages, where the material flow differs significantly from one another. With the optimum die scheme, the maximum stress and deflection of the extrusion die are both within the permitted ranges.
3. A real extrusion die is manufactured to verify the die modification scheme and a practical profile is produced on an 80 MN extrusion machine. By comparison, the maximum difference between experimental measurements and desired thicknesses of the ribs is 0.12 mm, which satisfies the engineering requirements. Moreover, by examining the microstructures in the profile and its ribs, no heat defects are observed in the profile.

Acknowledgments The authors would like to acknowledge financial support from the National Natural Science Foundation of China (51105230, 51375270), China Postdoctoral Science Foundation (2014M560551), and National Science & Technology Pillar Program in the Eleventh Five-Year Plan Period of the People's Republic of China (2009BAG12A07-B01).

References

1. Reiso O (2004) Extrusion of AlMgSi alloys. Mater Forum 28:32–46
2. Koopman AJ (2008) Analysis tools for the design of aluminium extrusion dies. Dissertation, University of Twente
3. Lee JM, Kim BM, Kang CC (2005) Effects of chamber shapers of porthole die on elastic deformation and extrusion process in condenser tube extrusion. Mater Des 26:327–336
4. Peng Z, Sheppard T (2005) Effect of die pockets on multi-hole die extrusion. Mater Sci Eng A407:89–97
5. Kloppenborg T, Schwane M, Ben Khalifa N, Tekkaya AE, Brosius A (2012) Experimental and numerical analysis of material flow in porthole die extrusion. Key Eng Mater 491:97–104
6. Carmai SJJ, Pitakthapanaphong S, Sechjarern S (2008) 3D finite element analysis of metal flow in hot aluminium extrusion of T-shaped profile with various offset pockets. J Achiev Mater Manuf Eng 31:463–468
7. Donati L, Tomesani L, Shikorra M (2009) The effect of pocket shape in extrusion dies. Int J Mater Form 2:97–100
8. He YF, Xie SS, Cheng L, Huang GJ, Fu Y (2010) FEM simulation of aluminum extrusion process in porthole die with pockets. Trans Nonferrous Metals Soc China 20:1067–1071
9. Fang G, Zhou J, Duczczyk J (2010) FEM-assisted design of a multi-hole pocket die to extrude U-shaped aluminum profiles with different wall thicknesses. Key Eng Mater 424:213–220
10. Chen H, Zhao GQ, Zhang CS, Liu JW (2011) Effects of welding chamber step on extrusion process of a complex hollow profile. Adv Mater Res 148–149:1684–1688
11. Chen H, Zhao GQ, Zhang CS, Wen DS (2011) Effects of multi-step welding chamber on extrusion product quality and die strength. Appl Mech Mater 44–47:311–315
12. Zhang CS, Zhao GQ, Sun XM, Chen H, Gao BJ (2011) Optimization design of baffle plates in porthole die for aluminum profile extrusion. J Mater Des Appl 225:255–265
13. Li F, Jin JF, Guan J, Liu XJ (2009) Effect of inner cone punch on metal flow in extrusion process. Int J Adv Manuf Technol 42:489–496
14. Rout AK, Maity K (2011) Numerical and experimental study on the three-dimensional extrusion of square section from square billet through a polynomial-shaped curved die. Int J Adv Manuf Technol 54:495–506
15. Hwang YM, Chen JM (2013) Surface permeation and die design during rod extrusion processes. Int J Adv Manuf Technol 69:397–403
16. Liu P, Xie SS, Cheng L (2012) Die structure optimization for a large, multi-cavity aluminum profile using numerical simulation and experiments. Mater Des 36:152–160
17. Lof L, Blokhuis Y (2002) FEM simulations of the extrusion of complex thin-walled aluminium sections. J Mater Process Technol 122:344–354
18. HyperXtrude 10.0 manual, Altair Engineering, Inc.